

Supplementary Materials: A Review of Modeling Bioelectrochemical System: Engineering and Statistical Aspects

Shuai Luo, Hongyue Sun, Qingyun Ping, Ran Jin and Zhen He

Model Selection

To select an appropriate type of model, one can pick from a family of models, such as linear models, based on the problem under study, and then perform the model diagnostic to check model adequacy. If the residual plots suggest that the linear model is not adequate to model the data set under study, one can pick a different kind of model format. For instance, the residual plot in Figure S1a is generated by fitting an underlying quadratic model with a simple linear regression model. The figure shows there is a lack of fit, and some nonlinear trend is overlooked by the simple linear regression model. Therefore, a quadratic term can be added. Figure S1b shows that a quadratic model is adequate for the problem under study. Such a procedure can be repeated until an adequate model is obtained. If the linear models do not fit the data well, the more complex models such as nonlinear models and data mining models can be tried.

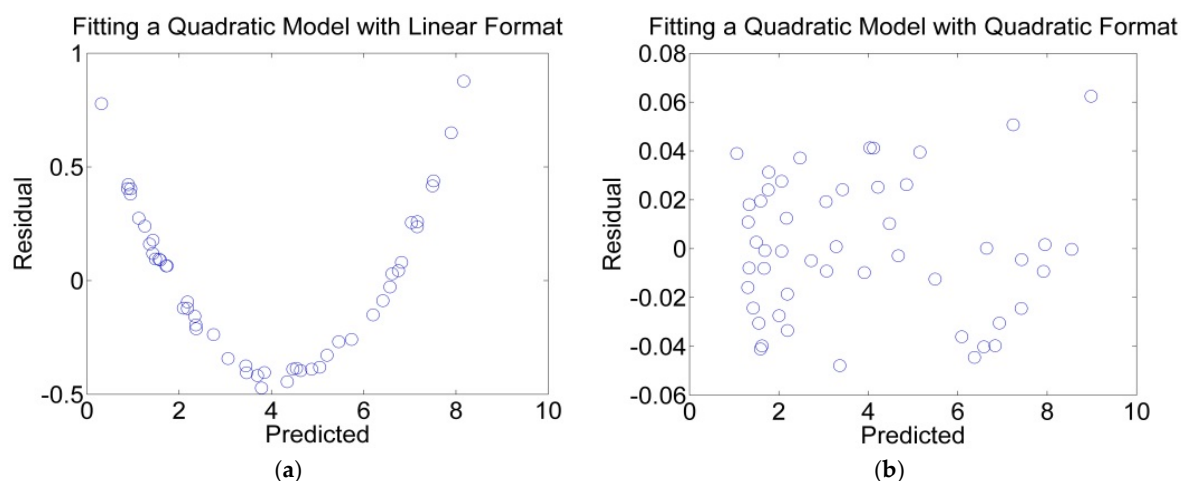


Figure S1. Use residual plot to determine model format. (a) Residual plot for fitting a underlying quadratic model with a simple linear regression model; and (b) residual plot for fitting a underlying quadratic model with a quadratic mode.

Table S1. General stereotype ODE.

Main Equations	Applications	Assumption (All in Reference)	Founders
$\frac{dX_B}{dt} = \frac{\phi}{v_B} (X_{in} - X_B) + r_{X,B} + r_{det} \frac{A_F}{v_B} - r_{ata} \frac{A_F}{v_B}$ $\frac{dS_B}{dt} = \frac{\phi}{v_B} (S_{in} - S_B) + r_{S,B} + \frac{1}{v_B} \int_{v_F} r_{S,F} dV + \frac{1}{v_B} \int_{A_F} r_{S,E} dA$ <p>(Assumption: F,G) X_B: biomass concentration; X_{in}: initial biomass concentration in bulk liquid; ϕ: influent liquid flow rate (zero in batch mode); v_B: bulk liquid volume; $r_{X,B}$: net biomass growth rate in the bulk; A_F: anode surface; r_{det}: biofilm detachment rate; r_{ata}: biofilm attachment rate; S_B: solute concentration; $r_{S,B}$: net substrate reaction rate in the bulk; $r_{S,F}$: net substrate reaction rate in the biofilm; $r_{S,E}$: electrochemical rates of solute component change on the electrode surface</p>	Predict concentration of microorganisms and soluble components in bulk liquid based on mass balance	A,C,D,E,F,G	Picioreanu <i>et al.</i> [1]
$\frac{dS}{dt} = D(S_0 - S) - q_a X_a - q_m X_m$ $\frac{dX_a}{dt} = \mu_a X_a - K_{d,a} X_a - \alpha_a D X_a$ $\frac{dX_m}{dt} = \mu_m X_m - K_{d,m} X_m - \alpha_m D X_m$ <p>(Assumption: F,G) S: substrate concentration; S_0: influent substrate concentration; D: dilution rate ($D = \frac{Flow\ rate}{Volume}$); X_a: concentration of anodophilic microorganism; X_m: concentration of methanogenic microorganism; q_a, q_m: substrate consumption rates of anodophilic and methanogenic microorganism; μ_a, μ_m: growth rates of anodophilic and methanogenic microorganism; $K_{d,a}, K_{d,m}$: decay rate of anodophilic and methanogenic microorganism; α_a, α_m: dimensionless biofilm retention constants of anodophilic and methanogenic microorganism</p>	Predict the concentration of targeted substrate, anodophilic and methanogenic microorganisms, and embody the competition between these two kinds of microorganisms	A,C,D,F,G,I	Pinto <i>et al.</i> [2]
$\frac{dM_{ox}}{dt} = -Y q_a + \gamma \frac{I_{MFC}}{mF} \frac{1}{V X_a}$ (Assumption: C) $\mu_a = \mu_{max,a} \frac{S}{K_{S,a} + S} \frac{M_{ox}}{K_M + M_{ox}}$ (Assumption: H) M_{ox} : oxidized mediator fraction per anodophilic microorganism; Y : mediator yield; q_a : substrate consumption rate of anodophilic organism; γ : mediator molar mass; I_{MFC} : MFC current; m : number of electrons transferred per mol of mediator; F : Faraday constant; V : bulk liquid volume; X_a : concentration of anodophilic microorganism; $\mu_a, \mu_{max,a}$: growth rate and maximum growth rate of anodophilic microorganism; S : substrate concentration; $K_{S,a}, K_M$: half-saturation (Monod) constant	Predict the impact of mediator to carry electrons from oxidizer to reducer to achieve the current generation	A,C,D,F,G,H,I	Pinto <i>et al.</i> [2,3]

Note: capital letter in assumption column refers to Table S3.

Table S2. Applications of ODE in MFC modeling.

Stereotype ODE Source	Equation Addition or modification on Stereotype (Only show important equations and assumptions)	Application	Assumption (All in Reference)	Reference
Pinto <i>et al.</i>	$\frac{dC_{salt,m}}{dt} = D_{salt}(C_{salt,in} - C_{salt,m}) - d(C_{salt,m} - C_{salt,a}) - d(C_{salt,m} - C_{salt,c}) - \frac{I_{MDC}}{F * V_{salt}}$ $\frac{dC_{salt,a}}{dt} = d(C_{salt,m} - C_{salt,a}) - DC_{salt,a}$ $\frac{dC_{salt,c}}{dt} = d(C_{salt,m} - C_{salt,c})$ <p>(Assumption: F,L) $C_{salt,m}, C_{salt,a}, C_{salt,c}$: salt concentrations in the salt, anode, and cathode compartments; D_{salt}: dilution rate in salt chamber ($D_{salt} = \frac{Q_{flow,salt,m}}{V_{salt}}$); d: membrane salt transfer coefficient ($d = \frac{f * A}{b * V_a}$, f: diffusion coefficient; A: membrane surface area; b: membrane thickness; V_a: anode volume); I_{MDC}: current through the circuit of MDCs; V_{salt}: volume of salt chamber.</p>	Estimate the salt concentration under various conditions to optimize MDC performance	A,C,D,F,G,H,L	[4,5]
Pinto <i>et al.</i>	$\frac{dC_{salt,a}}{dt} = \frac{Q_{anode,in}}{V_{anode}} C_{salt,a,in} - \frac{Q_{anode,out}}{V_{anode}} C_{salt,a} - \frac{J_s}{V_{anode}} A_m$ $\frac{dC_{salt,c}}{dt} = \frac{Q_{anode,in}}{V_{cathode}} C_{salt,c,in} - \frac{Q_{cathode,out}}{V_{cathode}} C_{salt,c} + \frac{J_s}{V_{anode}} A_m$ <p>(Assumption: F) $C_{salt,a}, C_{salt,c}$: salt concentration in the anode and cathode; $C_{salt,a,in}, C_{salt,c,in}$: salt concentration in the anode and cathode influent; $Q_{anode,in}, Q_{anode,out}$: influent and effluent flow rate; $V_{anode}, V_{cathode}$: volume of anode and cathode; J_s: reverse salt flux; A_m: membrane area.</p>	Estimate the impact of water flux through forward osmosis (FO) on the performance of entire system	A,C,D,F,G,H,J	[6]
Pinto <i>et al.</i>	$\frac{dm}{dt} = Q_{out}X - J_{air}m\beta \frac{m}{K_{air} + m}$ $\frac{d\beta}{dt} = \gamma\beta$ <p>(Assumption: F) m: cake layer mass; Q_{out}: effluent rate; X: concentration of suspended solids; J_{air}: air cross-flow; β: resistance of the cake to detachment; K_{air}: half-saturation coefficient of air flow; γ: coefficient for cake detachment.</p>	Predict the the dynamic change of biomass “cake” on the microbial membrane reactor	C,D,F,H	[7]
Picioareanu <i>et al.</i>	$A_{ano}Z \frac{dC_{i-glu}}{dt} = A_{ano} \frac{D_{glu}}{Z} (C_{i-1-glu} - C_{i-glu})$ $A_{ano}Z \frac{dC_{i-H^+}}{dt} = A_{ano} \frac{D_{H^+}}{Z} (C_{i+1-H^+} - C_{i-H^+}) - A_{ano} \frac{D_{H^+}}{Z} (C_{i-H^+} - C_{i-1-H^+}) + 2R_{Ai-glu}A_{ano} + 7R_{Ai-ace}A_{ano}Z + 13R_{Ai-pro}A_{ano}Z + 2 * 0.29R_{Ai-H_2}A_{ano}Z$ <p>(Assumption: B,K) $C_{i-glu}, C_{i-1-glu}$: glucose concentration in i^{th} and $(i-1)^{th}$ layer, A_{ano}: surface are of anode electrode; Z: biofilm thickness; $R_{Ai-glu}, R_{Ai-ace}, R_{Ai-pro}, R_{Ai-H_2}$: local consumption rates of glucose, acetate, propionate and hydrogen in each finite layer; D_{glu}, D_{H^+}: Diffusion coefficient of glucose and proton</p>	Finite difference approach is applied to divide biofilm into multiple finite layers to predict chemical kinetics of glucose and proton between biofilm and bulk solution	B,D,I,K	[8]

Note: capital letter in assumption column refers to Table S3.

Table S3. Assumption Lists for ODE modeling.

Assumption Letter	Assumptions	Limitations to be Solved by Assumption
A	Simple substrate (<i>i.e.</i> , acetate) is chosen to be electron donor and carbon source due to complete degradation to CO ₂ .	Uncertainty exists for the reaction rate for step-by-step degradation of complex substrate[9]. Acetate takes only one step of degradation to produce CO ₂ to make model available.
B	Glucose degradation is assumed to have two main designed steps with fixed chemical reactions to only produce hydrogen, acetate and propionate.	Uncertainty exists for products from the degradation of glucose [10]. Two-degradation eliminates the uncertainty.
C	Certain concentration of redox mediator exists from the beginning in the bulk liquid, and redox mediator produced by anodophilic microorganism completes electron transfers in the model.	Different electron transferring mechanisms may exist for anodophilic bacteria [11]. Assumption of only one electron transferring mechanism to work can eliminate the interference of other mechanisms in the model.
D	Constant value of cathode potential is set due to model focus on anode chamber.	The model focuses on the problem of anode. Eliminating the limitation of cathode can reduce the external interference on anode performance.
E	Ammonium is chosen to be nitrogen source.	Ammonia is common nutrient for the bacteria to utilize [12–14]. To eliminate the interference of other nitrogen type, ammonia is assumed to be nitrogen source.
F	Substrate and microorganism in the bulk solution and electrode biofilm are assumed to be ideally mixed or uniform.	Distance to the electrode and substrate distribution has effect on system performance. Assumption can reduce the interference and overcome the model limitation.
G	Acetate can feed two competing microbial populations independently, anodophilic and methanogenic bacteria. Growth rate and methane production of methanogenic bacteria depends on acetate concentration.	Multiple types of bacteria and substrate complicates the reaction kinetics, and model cannot simulate the substrate degradation and growth of all bacteria. Classification of only two types of bacteria can overcome the model limitation.
H	Multiplicative Monod kinetics is used to describe growth kinetics of anodophilic microorganisms, whose growth rate depends on acetate and intracellular mediator.	Multiplicative Monod kinetics can simplify and control the limiting factors for the impact on growth rate of bacteria, to make model workable.
I	Temperature or pH is considered fully controlled and kept constant (not the limiting factor in the system).	pH and temperature can influence the system environment and reaction kinetics, to finally influence the substrate degradation. Keeping constant of temperature and pH can eliminate the influence of these two factors to make model workable.
J	Anodophilic microorganism is the dominant community.	Multiple bacteria exist in the system, and setting anodophilic microorganisms as dominant community is to use the model to simulate the impact of anodophilic microorganisms in electricity generation, since other bacteria are unimportant and relatively rare.
K	Consumption rate of substrate in the bulk liquid is assumed to be negligible relatively to consumption rate within the electrode biofilm.	To simulate the degradation rate of substrate throughout the biofilm, the substrate degradation in the bulk solution should be neglected to reduce the interference of bulk solution on the system.
L	Electromigration of every electron between two electrodes pulls out a salt ion from salt chamber.	Since the salt is sodium chloride (NaCl) in the experiment, the assumption is reasonable because Na ⁺ and Cl ⁻ are monovalent ion. The assumption that electromigration of every electron pulls a salt ion facilitates the mathematical calculation for the problem.

Table S4. General stereotype PDE equations.

Main Equations	Applications	Assumptions (All in Reference)	Founders
$0 = \kappa_{bio} \frac{\partial^2 \eta}{\partial z^2} - \frac{FY_1}{\tau} f e^0 X_{f,a} q - \frac{FY_2}{\tau} X_{f,a} r_{res}$ $j = -k_{bio} \frac{d\eta}{dz}$ <p>(Assumption: A,C,G) η: local potential; z: biofilm distance; κ_{bio}: biofilm conductivity; F: diffusion coefficient; $X_{f,a}$: the density of active biomass; q: specific rate of electron donor utilization; j: current density; γ_1: electron equivalence of electron donor; γ_2: electron equivalence of active biomass (based on an empirical formula for microbial cells, $C_5H_8N_2O_6$ [15]); τ: time conversion; $f e^0$: fraction of electrons from the electron donor used for energy generation to support synthesis; r_{res}: biomass respiration rate</p>	Predict dynamics of the biofilm growth and the electrical conduction on the anode	A,B,C,D,E,F,G	Marcus <i>et al.</i> [16]
$f_1(x) = -D_{i,m} \frac{\partial c_i(x)}{\partial x} + \frac{z_i F}{RT} D_{i,m} c_i(x) \phi(x)$ <p>(Assumption: I) $D_{i,m}$: diffusion coefficient of an ion species i; $c_i(x)$: concentration of ion species i at distance x; x: distance in the ion exchange membrane; z_i: number of electrons transferred by ion species i; F: Faraday constant; R: universal gas constant; T: temperature; $\phi(x)$: electric field at the distance x in the ion exchange membrane</p>	Integrate Nernst-Planck equation together to predict various ion flux through the ion exchange membrane	H,I	Harnisch <i>et al.</i> [17]
$\frac{\partial S_F}{\partial t} = \frac{\partial}{\partial x} \left(D \frac{\partial S_F}{\partial x} \right) + \frac{\partial}{\partial y} \left(D \frac{\partial S_F}{\partial y} \right) + \frac{\partial}{\partial z} \left(D \frac{\partial S_F}{\partial z} \right) + r_{S,F}$ <p>(Assumption: J,M) S_F: solute concentration on the biofilm; $\frac{\partial S_F}{\partial x}, \frac{\partial S_F}{\partial y}, \frac{\partial S_F}{\partial z}$: spatial concentration gradient for solute component; $r_{S,F}$: net reaction rate of soluble components; D: diffusion coefficient</p>	Predict soluble component on the biofilm, considering the substrate diffusion and spatial distribution of the microorganisms in biofilm	J,K,L,M,N	Picioreanu <i>et al.</i> [1]
$\frac{\partial C_{i,F}}{\partial t} = D_i \nabla^2 C_{i,F} + z_i u_{m,i} F \nabla (C_{i,F} \nabla V) - \mathbf{u} \nabla C_{i,F} + r_{i,F}$ $\frac{\partial \mathbf{u}}{\partial t} = -(\mathbf{u} \cdot \nabla) \mathbf{u} - \frac{1}{\rho} \nabla p + \nu \nabla^2 \mathbf{u}$ $\mathbf{u} \cdot \nabla = 0$ <p>(Assumption: O,P) $C_{i,F}$: concentration of solute component; D_i: diffusion coefficient of ion species i; $u_{m,i}$: ion mobilities ($u_{m,i} = \frac{D_i}{RT}$); z_i: charge of species i; ∇V: potential gradient; F: Faraday constant; \mathbf{u}: field of liquid velocity; p: pressure; ρ: density</p>	Introduce Nernst-Planck equation to predict the impact of pH and electrode geometry on the entire performance, considering diffusion, electromigration, and substrate consumption rate together	F,K,L,M,O,P	Picioreanu <i>et al.</i> [18]

Note: capital letter in assumption column refers to Table S6.

Table S5. Applications of PDE in MFC modeling.

Stereotype PDE Source	Equation Addition or Modification on Stereotype (Only show important additions)	Application	Assumption (All in Reference)	Reference
Marcus <i>et al.</i>	$\kappa_{bio} \frac{\partial^2}{\partial x^2} \eta - \frac{F}{\tau v} (\gamma_{e-suc} r_{exo} + \gamma_{e-b} r_{endo}) = 0$	Apply chemical kinetics to simulate concentration profiles of molasses and oxygen as a function of time and location through the entire MFC	B,C,Q,R	[19]
	(Assumption: B,C)			
	$\frac{\partial}{\partial t} [Suc]_{bio} = D_{suc,bio} \frac{\partial^2}{\partial z^2} [Suc]_{bio} - r_{exo}$ $\frac{\partial}{\partial t} [H^+]_{bio} = D_{H^+} \frac{\partial^2}{\partial z^2} [H^+]_{bio} + 60r_{exo}$			
Picioreanu <i>et al.</i>	(Assumption: C, Q)	Predict the the dynamic change of biomass “cake” on the microbial membrane reactor	A,C,G,M,K	[20,21]
	$\frac{\partial C_{F,X}}{\partial t} = - \frac{\partial (u_F C_{F,X})}{\partial x} + r_{bio,X}$ $C_{F,X}$: biomass concentration in the biofilm; u_F : convection velocity; $r_{bio,X}$: net biomass generation			
Harnisch <i>et al.</i>	$\frac{\partial c_i}{\partial t} = - \frac{\partial J_i}{\partial x} + \Gamma_i$ (Assumption: M,S,T) c_i : ion concentration of species i ; J_i : ionic flux of species i ; Γ_i : formation rate of species i	Describe the mass balance of ammonia and carbonate group in anode and cathode chamber	M,S,T	[22]

Note: capital letter in assumption column refers to Table S6.

Table S6. Assumption Lists for PDE modeling.

Assumption Letter	Assumption	Limitations to be Solved by Assumption
A	The biofilm matrix is a conductor characterized by the biofilm conductivity, and active and inert biomass on the biofilm shares the same biofilm conductivity.	Biofilm can conduct the electrons to the anode, and the concept of biofilm conductivity is to uniformize the biofilm for electron transferring, and conductivity can be set as a parameter to facilitate model calculation.
B	Active biomass transfers electrons to the conductive biofilm matrix as its only outlet for electrons generated in substrate and endogenous respirations.	Active biomass on the electrode can transfer extracellular electron to the anode for current generation [23]. This assumption is to eliminate the impact of other electron acceptors in the system.
C	The rate of donor-substrate utilization depends on the local concentration of the donor and/or the local potential.	This assumption is to embody the impact of substrate gradient on the substrate degradation rate in different regions on the biofilm. This assumption enables model to take spatial factors into account for modeling.
D	The biofilm is well connected to the electrode, without any overpotential in the charge-transfer reaction.	The model cannot simulate charge-transfer reaction. This assumption maintains that the electrons produced by biofilm can be completely received by the electrode. This eliminates the interference of charge-transfer reaction.
E	A non-limiting flow of anions and cations in the biofilm maintains electroneutrality.	This assumption is to make model fit the principle of electroneutrality in the solution system.
F	Temperature or pH is considered fully controlled and kept constant (not the limiting factor in the system).	pH and temperature can influence the system environment and reaction kinetics, to finally influence the substrate degradation. Keeping constant of temperature and pH can eliminate the influence of these two factors to make model workable.
G	The transfer of electron from the bacteria to the conductive biofilm matrix is rapid and reversible.	The model cannot predict the possible barrier between the electrons transferring from bacteria to the biofilm matrix. This assumption maintains that the electrons produced by bacteria can be completely transferred to the biofilm matrix. This assumption guarantees the fitting to the concept of biofilm conductivity.
H	An oxidation reaction takes place in anode, where one proton is released per liberated electron, and a reduction reaction takes place in cathode, where one proton is consumed per transferred electron.	The assumption fits the general electrochemical reaction in MFC and electroneutrality in the solution system that the production of one proton accompanies with the release of one electron. This assumption facilitates the calculation.
I	All ion concentrations are in equilibrium within anode and cathode.	This assumption fits the concept of solution electroneutrality, and the charge balance enables the calculation of the change of the ion concentration in the system.
J	Simple substrate (i.e., acetate) is chosen to be electron donor and carbon source due to complete degradation to CO ₂ .	Uncertainty exists for the reaction rate for step-by-step degradation of complex substrate [9]. Simple substrate can take only one step of degradation to produce CO ₂ to make model calculation available to be used.
K	Certain concentration of redox mediator exists from the beginning in the bulk liquid, and redox mediator produced by anodophilic microorganism completes electron transfers in the model.	Different electron transferring mechanisms may exist for anodophilic bacteria [11]. Assumption of only one electron transferring mechanism to work can eliminate the interference of other mechanisms in the model.
L	Constant potential of specific electrode is uniformly set, to eliminate the limiting factor caused by the electrode itself.	The model focuses on the problem of anode. Eliminating the limitation of cathode can reduce the external interference on anode performance, to make the model available for anode situation.
M	Substrate and microorganism in the bulk solution and electrode biofilm are assumed to be ideally mixed or uniform.	Distance to the electrode and substrate distribution has effect on system performance. Assumption can reduce the interference and overcome the model limitation.

N	Acetate can feed two competing microbial populations independently, anodophilic and methanogenic bacteria. Growth rate and methane production rate depends on acetate concentration.	Multiple types of bacteria and substrate complicates the reaction kinetics, and model cannot simulate the substrate degradation and growth of all bacteria. Classification of only two types of bacteria can overcome the model limitation.
O	Microscale domain chosen is representative for the whole biofilm developed on the electrode.	The model cannot calculate all output on every domain in the biofilm, and choosing a representative region to uniformize the entire biofilm is easy way to make the model work.
P	Constant diffusion coefficient, ion mobilities and incompressible fluid are assumed constant for setting the mass balance of soluble component.	This assumption is to eliminate the effect of diffusion, ion mobilities and fluid compressibility, to eliminate the impact of these factors on the model performance.
Q	Sucrose was assumed to be the main substrate for the MFC, consumed by the bacteria, localized and dispersed throughout the biofilm.	This research is to use sucrose as main carbon source, and this assumption is needed to focus on kinetic change of sucrose, to make model competent to simulate the change of sucrose.
R	The cathode was assumed to have a layer of polytetrafluoroethylene (PTFE), which is permeable to oxygen but not water.	This assumptions is to guarantee that PTFE is ideal layer without any barrier to oxygen diffusion, and it can guarantee system without water loss.
S	In the membrane and in solution all of the acid-base reactions (e.g., conversion from NH_4^+ to NH_3) are infinitely fast.	This assumption can guarantee the immediate conversion of ion species in the membrane and solution to reduce the impact of proton or base on the distribution of ion species.
T	Ions do not participate in any other (equilibrium) reaction in anode or cathode, and reactions in anode or cathode are infinitely faster than reaction in membrane.	This assumption is to eliminate the impact of anode and cathode reaction on the ion transportation through the membrane.

Table S7. Model error of engineering and statistical models

Model method (Evaluation method)	Application	Results (based on the reference)	Reference
ODE (MSE)	Model MFC performance (e.g., current generation and substrate degradation) under different operating conditions	MFC-4: Voltage: 3.2% Substrate: 5.3% Methane production: 2.7%	Pinto <i>et al.</i> [2]
ODE (R ²)	Model MEC performance (e.g., hydrogen and methane production) under different operating conditions	MEC-3: Effluent COD: 0.65 Effluent VFA: 0.70 Current: 0.82 H ₂ flow-cathode: 0.65 CH ₄ flow-cathode: 0.81 CH ₄ flow-anode: 0.57 Under different flow rates: Current: 6.97% Salt concentration: 12.12%:	Pinto <i>et al.</i> [3]
ODE (RMSE)	Analyze impact of multiple factors (e.g., organic concentration, external resistance, flow rate) on current generation, salt removal rate	Under different organic concentration: Current: 12.08% Salt concentration: 9.01% Current: 8.06% Water Flux: 31.95%	Ping <i>et al.</i> [4]
ODE (RMSE)	Model OsMFC performance under differently initial salt concentrations in the salt chamber	Salt concentration in anode and cathode: 3.19% and 7.17%	Qin <i>et al.</i> [6]
ODE (RMSE)	Model PRO-MEC performance under different operating conditions	PRO: Volume profile under different situations: <2.5% MEC: Externally supplied voltage 0.6 V: 16.5% 0.8 V: 13.0% 1.0 V: 23.6% Organic concentration: 357 mg/L: 12.1% 2007 mg/L: 21.6%	Yuan <i>et al.</i> [24]
ODE (RMSE)	Construct different models for MBER in various configurations to guide MBER development and optimization	MBER-1 Current: 15.2% (normal flow rate at 0.23 ml/min) Current: 20.8% (high flow rate at 0.39 ml/min) Current: 18.4% (back to normal flow rate at 0.23 ml/min) Transmembrane pressure (TMP): 11.3% (from days 20 to 66) and 5.4% (at final period)	Li <i>et al.</i> [7]

		MBER-2 TMP: 8.6% Total nitrogen: 9.7% Current: 24.8% MBER-3 Current: 8.8% (from days 10 to 43) and 55.7% (on day 63) TMP: 9.0%	
PDE (grid error and numerical error)	Model ion transfer across ion exchange membranes under BES	Computed potential values: <3% (grid error) and <1% (numerical error)	Harnisch <i>et al.</i> [17]
SLR (R ²)	1) Model current density with biochemical oxygen demand for different substrates, and 2) model current density with active microorganisms concentration for a submersible MFC	1) & 2) R ² > 0.96	Zhang and Angelidaki, [25]
SLR (R ²)	Model current with acetate concentration for an MFC biosensor	R ² = 0.92	Tront <i>et al.</i> [26]
SLR (R ²)	Model positive charge with negative charge for a two-chamber MFC	R ² = 0.99	Rozendal <i>et al.</i> [27]
ANOVA, RSM (R ²)	1) Model power density with pH and catholyte buffer concentration, and 2) model columbic efficiency with pH and catholyte buffer concentration for a two-chamber MFC	1) R ² = 0.93 2) R ² = 0.87	Madani <i>et al.</i> [28]
ANOVA, RSM (R ²)	Model COD removal, nitrogen removal and power density with pH, distance between electrodes and external resistance for a two-chamber MFC	R ² > 0.97	Sajana <i>et al.</i> [29]
MLM (RMSE)	Model normalized energy recovery and organic removal efficiency with design factors, operational factors and covariates for a five-module two-chamber MFC	RMSE < 9.50%	Sun <i>et al.</i> [30]
ANOVA, RSM (R ² and adjusted R ²)	Model power density and COD removal with pH, buffer concentration and ionic strength for a two-chamber MFC	R ² > 0.92, adjusted R ² > 0.86	Hosseinpour <i>et al.</i> [31]
ANOVA, RSM (R ² and adjusted R ²)	Model pentachlorophenol degradation, power density and columbic efficiency with glucose concentration, temperature and pH for an mediator-less single-chamber MFC	R ² > 0.94, adjusted R ² > 0.89	Al-Shehri [32]
ANOVA, RSM (R ² and adjusted R ²)	Model voltage with sucrose concentration, temperature and ferrous sulfate concentration for a two-chamber MFC	R ² = 0.97, adjusted R ² = 0.93	Jia <i>et al.</i> [33]
ANOVA, RSM (R ²)	Model short-chain fatty acid generation with carbon to nitrogen ratio, pH, temperature and hydraulic retention time for an membrane-less MFC	R ² > 0.99	Chen <i>et al.</i> [34]
ANOVA, RSM (R ²)	Model voltage with glucose, KCl and NaHCO ₃ for a two-chamber MFC	R ² = 0.92	Al-Shehri <i>et al.</i> [35]
GP, ANN, SVM (R ²)	Model voltage with temperature and ferrous sulfate concentration for a two-chamber MFC	R ² > 0.95	Garg <i>et al.</i> [36]
ANN (R ² and MSE)	Model power density with temperature, pH and electron acceptor concentration for an membrane-less MFC	R ² > 0.95, MSE > 0.97%	Tardast <i>et al.</i> [37]
RVM (R ² and RMSE)	Model columbic efficiency and power density with ionic strength, pH, medium nitrogen concentration and temperature for a two-chamber MFC	R ² < 0.97 RMSE: columbic efficiency (<0.16); power density: 48.2	Fang <i>et al.</i> [38]

MSE: mean square error; RMSE: root-mean-square error; R²: coefficient of determination (denoted as R squared).

References

- Picioreanu, C.; Head, I.M.; Katuri, K.P.; Van Loosdrecht, M.C.; Scott, K. A computational model for biofilm-based microbial fuel cells. *Water Res.* **2007**, *41*, 2921–2940.
- Pinto, R.P.; Srinivasan, B.; Manuel, M.F.; Tartakovsky, B. A two-population bio-electrochemical model of a microbial fuel cell. *Bioresour. Technol.* **2010**, *101*, 5256–5265.
- Pinto, R.; Srinivasan, B.; Escapa, A.; Tartakovsky, B. Multi-population model of a microbial electrolysis cell. *Environ. Sci. Technol.* **2011**, *45*, 5039–5046.
- Ping, Q.; Zhang, C.; Chen, X.; Zhang, B.; Huang, Z.; He, Z. Mathematical model of dynamic behavior of microbial desalination cells for simultaneous wastewater treatment and water desalination. *Environ. Sci. Technol.* **2014**, *48*, 13010–13019.
- Ping, Q.; Huang, Z.; Dosoretz, C.; He, Z. Integrated experimental investigation and mathematical modeling of brackish water desalination and wastewater treatment in microbial desalination cells. *Water Res.* **2015**, *77*, 13–23.
- Qin, M.; Ping, Q.; Lu, Y.; Abu-Reesh, I.M.; He, Z. Understanding electricity generation in osmotic microbial fuel cells through integrated experimental investigation and mathematical modeling. *Bioresour. Technol.* **2015**, *195*, 194–201.
- Li, J.; He, Z. Development of a dynamic mathematical model for membrane bioelectrochemical reactors with different configurations. *Environ. Sci. Pollut. Res. Int.* **2015**, *23*, 3897–3906.
- Zhang, L.; Deshusses, M. Application of the finite difference method to model pH and substrate concentration in a double-chamber microbial fuel cell. *Environ. Technol.* **2014**, *35*, 1064–1076.
- Wang, Y.; Zhang, Y.; Wang, J.; Meng, L. Effects of volatile fatty acid concentrations on methane yield and methanogenic bacteria. *Biomass Bioenergy* **2009**, *33*, 848–853.
- Fang, H.H.; Liu, H. Effect of pH on hydrogen production from glucose by a mixed culture. *Bioresour. Technol.* **2002**, *82*, 87–93.
- Schroder, U. Anodic electron transfer mechanisms in microbial fuel cells and their energy efficiency. *Phys. Chem. Chem. Phys.* **2007**, *9*, 2619–2629.
- Stratford, J.; Dias, A.E.O.; Knowles, C.J. The utilization of thiocyanate as a nitrogen source by a heterotrophic bacterium: the degradative pathway involves formation of ammonia and tetrathionate. *Microbiology* **1994**, *140*, 2657–2662.
- Kondorosi, A.; Svab, Z.; Kiss, G.; Dixon, R. Ammonia assimilation and nitrogen fixation in *Rhizobium meliloti*. *Mol. Gen. Genet. MGG* **1977**, *151*, 221–226.
- Tolley-Henry, L.; Raper, C.D. Utilization of Ammonium as a Nitrogen Source Effects of Ambient Acidity on Growth and Nitrogen Accumulation by Soybean. *Plant Physiol.* **1986**, *82*, 54–60.
- McCarty, P.; Rittmann, B. *Environmental Biotechnology: Principles and Applications*; McGraw-Hill Education: New York, NY, USA, 2001.
- Marcus, A.K.; Torres, C.I.; Rittmann, B.E. Conduction-based modeling of the biofilm anode of a microbial fuel cell. *Biotechnol. Bioeng.* **2007**, *98*, 1171–1182.
- Harnisch, F.; Warmbier, R.; Schneider, R.; Schröder, U. Modeling the ion transfer and polarization of ion exchange membranes in bioelectrochemical systems. *Bioelectrochemistry* **2009**, *75*, 136–141.
- Picioreanu, C.; van Loosdrecht, M.C.; Curtis, T.P.; Scott, K. Model based evaluation of the effect of pH and electrode geometry on microbial fuel cell performance. *Bioelectrochemistry* **2010**, *78*, 8–24.
- Sirinutsomboon, B. Modeling of a membraneless single-chamber microbial fuel cell with molasses as an energy source. *Int. J. Renew. Energy Environ. Eng.* **2014**, *5*, 1–9.
- Korth, B.; Rosa, L.F.; Harnisch, F.; Picioreanu, C. A framework for modeling electroactive microbial biofilms performing direct electron transfer. *Bioelectrochemistry* **2015**, *106*, 194–206.
- Wang, C.-T.; Shaw, C.K.; Hu, T.-Y. Optimization of flow in microbial fuel cells: an investigation into promoting micro-mixer efficiency with obstacle. *Tamkang J. Sci. Eng.* **2011**, *14*, 25–31.
- Dykstra, J.; Biesheuvel, P.; Bruning, H.; Ter Heijne, A. Theory of ion transport with fast acid-base equilibrations in bioelectrochemical systems. *Phys. Rev. E* **2014**, *90*, doi:10.1103/PhysRevE.90.013302.
- Carmona-Martínez, A.A.; Harnisch, F.; Kuhlicke, U.; Neu, T.R.; Schröder, U. Electron transfer and biofilm formation of *Shewanella putrefaciens* as function of anode potential. *Bioelectrochemistry* **2013**, *93*, 23–29.
- Yuan, H.; Lu, Y.; Abu-Reesh, I.M.; He, Z. Bioelectrochemical production of hydrogen in an innovative pressure-retarded osmosis/microbial electrolysis cell system: Experiments and modeling. *Biotechnol. Biofuels* **2015**, *8*, 116.

25. Zhang, Y.; Angelidaki, I. Submersible microbial fuel cell sensor for monitoring microbial activity and BOD in groundwater: focusing on impact of anodic biofilm on sensor applicability. *Biotechnol. Bioeng.* **2011**, *108*, 2339–2347.
26. Tront, J.M.; Fortner, J.D.; Plotze, M.; Hughes, J.B.; Puzrin, A.M. Microbial fuel cell biosensor for *in situ* assessment of microbial activity. *Biosens. Bioelectron.* **2008**, *24*, 586–590.
27. Rozendal, R.A.; Hamelers, H.V.; Buisman, C.J. Effects of membrane cation transport on pH and microbial fuel cell performance. *Environ. Sci. Technol.* **2006**, *40*, 5206–5211.
28. Madani, S.; Gheshlaghi, R.; Mahdavi, M.A.; Sobhani, M.; Elkamel, A. Optimization of the performance of a double-chamber microbial fuel cell through factorial design of experiments and response surface methodology. *Fuel* **2015**, *150*, 434–440.
29. Sajana, T.K.; Ghangrekar, M.M.; Mitra, A. Effect of operating parameters on the performance of sediment microbial fuel cell treating aquaculture water. *Aquacult. Eng.* **2014**, *61*, 17–26.
30. Sun, H.; Luo, S.; Jin, R.; He, Z. Multitask Lasso Model for Investigating Multimodule Design Factors, Operational Factors, and Covariates in Tubular Microbial Fuel Cells. *ACS Sustain. Chem. Eng.* **2015**, *3*, 3231–3238.
31. Hosseinpour, M.; Vossoughi, M.; Alemzadeh, I. An efficient approach to cathode operational parameters optimization for microbial fuel cell using response surface methodology. *J. Environ. Health Sci. Eng.* **2014**, *12*, 33.
32. Al-Shehri, A. Statistical optimization of pentachlorophenol biodegradation and electricity generation simultaneously in mediator-less air cathode microbial fuel cell. *J. Environ. Appl. Biores.* **2015**, *3*, 6–15.
33. Jia, Q.; Wei, L.; Han, H.; Shen, J. Factors that influence the performance of two-chamber microbial fuel cell. *Int. J. Hydrog. Energy* **2014**, *39*, 13687–13693.
34. Chen, Y.; Luo, J.; Yan, Y.; Feng, L. Enhanced production of short-chain fatty acid by co-fermentation of waste activated sludge and kitchen waste under alkaline conditions and its application to microbial fuel cells. *Appl. Energy* **2013**, *102*, 1197–1204.
35. Al-Shehri, A.N.; Ghanem, K.M.; Al-Garni, S.M. Statistical Optimization of Medium Components to Enhance Bioelectricity Generation in Microbial Fuel Cell. *Arab. J. Sci. Eng.* **2012**, *38*, 21–27.
36. Garg, A.; Vijayaraghavan, V.; Mahapatra, S.S.; Tai, K.; Wong, C.H. Performance evaluation of microbial fuel cell by artificial intelligence methods. *Expert Syst. Appl.* **2014**, *41*, 1389–1399.
37. Tardast, A.; Rahimnejad, M.; Najafpour, G.; Ghoreyshi, A.; Premier, G.C.; Bakeri, G.; Oh, S.-E. Use of artificial neural network for the prediction of bioelectricity production in a membrane less microbial fuel cell. *Fuel* **2014**, *117*, 697–703.
38. Fang, F.; Zang, G.-L.; Sun, M.; Yu, H.-Q. Optimizing multi-variables of microbial fuel cell for electricity generation with an integrated modeling and experimental approach. *Appl. Energy* **2013**, *110*, 98–103.